Acta Geologica Polonica, Vol. 72 (2022), No. 2, pp. 145–158
DOI: 10.24425/agp.2021.139306

A silicoflagellate plexus associated with *Bachmannocena diodon* subsp. *nodosa* from the Eastern Equatorial Pacific (Ocean Drilling Program Leg 138)

ADRIANNA SZARUGA[1], KEVIN McCARTNEY[2]* and JAKUB WITKOWSKI[1]

[1] *Institute of Marine and Environmental Sciences, University of Szczecin, Mickiewicza 16a, 70-383 Szczecin, Poland.*
[2] *Department of Environmental Studies and Sustainability, University of Maine at Presque Isle, Presque Isle, ME 04769 USA. E-mail: kevin.mccartney@maine.edu*
* *Corresponding author*

ABSTRACT:

Szaruga, A., McCartney, K. and Witkowski, J. 2022. A silicoflagellate plexus associated with *Bachmannocena diodon* subsp. *nodosa* from the Eastern Equatorial Pacific (Ocean Drilling Program Leg 138). *Acta Geologica Polonica*, **72** (2), 145–158. Warszawa.

Upper Miocene (~6 Ma) sediments from a north-south transect of Ocean Drilling Program Holes 848B, 849B, 850B, 851B across the equator in the Eastern Pacific Ocean record an episode of unusual skeletal variability associated with the silicoflagellate *Bachmannocena diodon* subsp. *nodosa* (Bukry) Bukry, 1987. Skeletons in this plexus persisted for between 55,000 and 75,000 years and include an arch across a 2-sided basal ring, a highly unusual morphology for the genus. Groups of skeletal morphotypes were common within the plexus episode, and occur in a systematic sequence that is consistent between sites. As a result of this study, silicoflagellates previously placed in the genus *Neonaviculopsis* Locker and Martini, 1986 are now considered part of the *Bachmannocena diodon* subsp. *nodosa* plexus.

Key words: Silicoflagellates; Miocene; Morphological variability; Messinian; *Bachmannocena*; *Neonaviculopsis*.

INTRODUCTION

Skeletal plasticity makes silicoflagellate taxonomy a particularly challenging subject for study. Unusual skeletal variability occurs in living populations associated with low salinities (Takahashi *et al.* 2009) and rapid ecologic change (Malinverno *et al.* 2019). Abundant silicoflagellate teratoidism occurs among specimens collected from within sponges (Frenguelli 1935) and broad skeletal variety is present in a coastal embayment that received considerable volumes of freshwater influx (Shitanaka 1983, fig. 6). Such occurrences are, however, unusual and seldom observed in the open ocean, where silicoflagellates generally exhibit only occasional and inconsistent skeletal variation within taxa that often persist over millions of years (myr).

Another aspect of silicoflagellate variability is the presence of plexus episodes, where a range of specific and unusual skeletal morphologies occurs in large abundance within a single taxon, typically over a period of several 10s of thousand years (kyr). The 'plexus' term was first applied to silicoflagellates by McCartney and Wise (1990) to pseudofibulid varieties of *Stephanocha speculum* subsp. *speculum* (Ehrenberg) McCartney and Jordan in Jordan and McCartney, 2015 that were often dominant in late Miocene high southern latitudes (McCartney and Wise

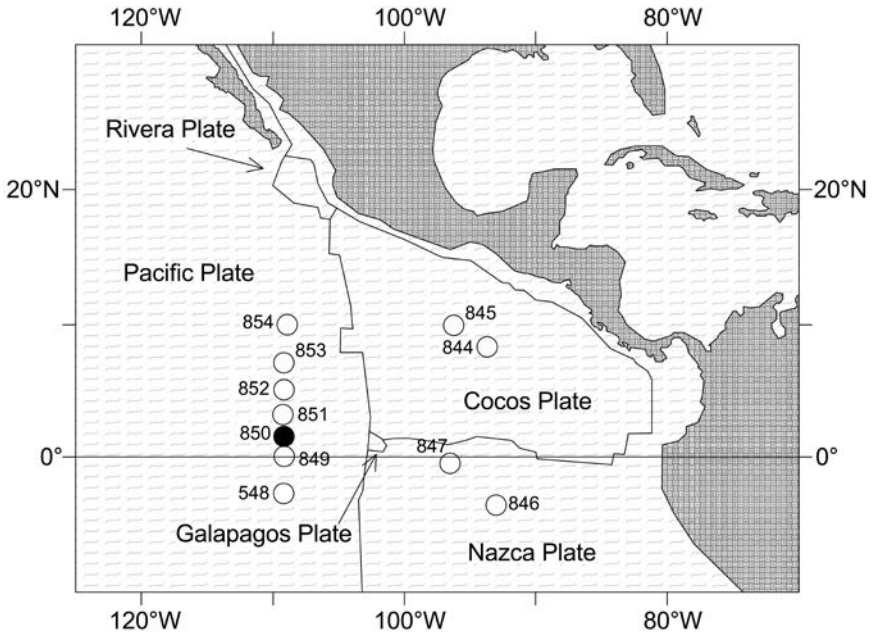

Text-fig. 1. Map of Leg 138 site locations. Holes in which the BDN plexus episode was observed are shown by solid circles, with locations of other sites from Leg 138 shown by open circles.

1993). This plexus includes three skeletal morphogroups with apically bridged (dictyochid) rather than the apically ringed designs more typically observed for *Stephanocha* McCartney and Jordan in Jordan and McCartney, 2015. Similar assemblages of pseudofibulid shapes have been observed among middle Eocene *Dictyocha grandis* Shaw and Ciesielski, 1983 (see also McCartney and Harwood 1992; Witkowski *et al.* 2012) and Upper Cretaceous *Arctyocha balkwillii* McCartney, Witkowski and Harwood, 2011.

A silicoflagellate plexus episode composed of different skeletal morphologies occurs in the Eastern Equatorial Pacific (EEP) upper Miocene (~6 Ma). This was first identified as a plexus by McCartney *et al.* (1995) in Ocean Drilling Program (ODP) Holes 848B, 849B, 850B and 851B positioned along a N-S transect (longitude ~110ºW), with less abundant plexid skeletons in Hole 847B located 15º to the east (Text-fig. 1). These diverse plexid skeletal morphologies have a range of naviculopsid morphologies (McCartney *et al.* 2020) associated with *Bachmannocena diodon* subsp. *nodosa* (Bukry) Bukry, 1987 (hereafter referred to as BDN; McCartney *et al.* 1995) and include a highly unusual arch across the 2-sided basal ring. These plexids were not observed at Holes 844B and 852B, located further from the equator (for information on these seven holes, see Table 1).

Hole	Latitude (°N or °S)	Longitude (°W)	Water depth (m)
844B	07°55.279'N	99°28.846'	3414.5
847B	00°11.593'N	95°19.227'	3334.3
848B	02°59.634'S	110°28.791'	3855.6
849B	00°10.983'N	110°31.183'	3839.1
850B	01°17.827'N	110°31.183'	3786.3
851B	02°46.223'N	110°04.308'	3760.3
852B	05°17.566'N	110°35.579'	3859.9

Table 1. Information on the seven ODP Leg 138 Holes examined as part of this study.

The purpose of this study is a reexamination of BDN plexid occurrences at high temporal resolution to: 1) better constrain the initiation and cessation of the plexus episode; 2) determine whether the skeletal morphotypes within a silicoflagellate plexus display any stratigraphic pattern (see McCartney and Wise 1990; McCartney *et al.* 1995; Witkowski *et al.* 2012); and 3) set the BDN plexus into a paleoceanographic context.

TAXONOMY OF THE *BACHMANNOCENA DIODON* SUBSP. *NODOSA* PLEXUS MEMBERS

The genus *Bachmannocena* Locker, 1974 (sometimes called *Mesocena* Ehrenberg, 1843) is characterized by the absence of any apical structure. This genus is phylogenetically distinct from the large and often many-spined *Paramesocena* Locker and

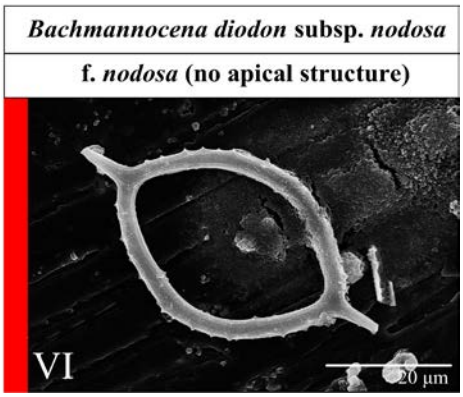

Text-fig. 2. SEM photograph of a representative *Bachmannocena diodon* subsp. *nodosa* skeleton (no apical structure, morphotype VI). The red color to the left indicates the predominance of this morphotype in Tables 3 to 7.

Martini, 1986 of middle to late Miocene age (Locker and Martini 1986), and from Cretaceous *Arctyocha mesocena* McCartney, Witkowski and Harwood, 2011. *Bachmannocena* skeletons usually measure 20–60 µm and have ovoid, trigonal or square/rhomboid shapes. A common *Bachmannocena* taxon from middle Miocene to lower Pliocene (nannoplankton zones NN5 to NN15, Locker and Martini 1986) is *B. diodon* subsp. *diodon* (Ehrenberg) Bukry, 1987 (hereafter BDD), which usually has an ovoid basal ring of moderate to large size (~45–70 µm) with two spines at near opposite ends of the major axis.

Bachmannocena diodon subsp. *nodosa* (Text-fig. 2) is usually of smaller size (~15–25 µm) but otherwise has a basal ring and surface texture similar to BDD. Plexid skeletons associated with BDN (McCartney *et al.* 1995) have been previously placed in three genera and past interpretations of these taxa are listed in Table 2. These skeletons include an arch across the two basal sides and occur as four morphogroups: 1) elongate basal rings of aspect ratio > 2:1 (f. *neonautica*); 2) ovid skeletons with arch location roughly equidistant to the two corners (f. *cocosensis*); 3) ovid skeletons with arch located closer to one corner (f. *transenna*); and 4) uncommon skeletons that have a bridge supported by struts (f. *praenautica*). The first three morphogroups occurred abundantly in various sediment samples and are illustrated in Text-fig. 3, while those of the fourth morphogroup were rarely observed.

The presentation of BDN plexid taxa as forms is consistent with the *Stephanocha speculum* pseudofibulid plexids in McCartney and Wise (1990) and McCartney and Harwood (1992), and *Bachmannocena diodon* morphologies observed in Locker and Martini

Paper	Leg	Hole	Location	Longitude, latitude	Water depth (m)	Taxon identification	Illustrated	This paper
Bukry and Foster (1973)	16	158	EEP	06°37.36'N, 85°14.16'W	1953	*Dictyocha navicula*	pl. 3, figs 6, 7	*B. d. n.* f. *neonautica*
						D. navicula	pl. 3, fig. 8	*B. d. n.* f. *cocosensis*
Bukry (1980)	54	425	EEP	01°23.68'N, 86°04.22'W	2850	*D.* sp. (naviculopsoid)	pl. 5, fig. 11	*B. d. n.* f. *cocosensis*
						D. sp. (naviculopsoid)	pl. 5, fig. 12	*B. d. n.* f. *neonautica*
Bukry (1981b)			Synthesis			*D. neonautica* n. sp.		
Bukry (1981a)	63	471	off Baja California	23°28.93'N, 112°29.78'W	3101	*D. n.* var. *cocosensis* n. var.	pl. 3, figs 1-3	*B. d. n.* f. *cocosensis*
						D. neonautica neonautica	pl. 3, fig. 4	*B. d. n.* f. *neonautica*
Bukry (1982a)	67	495	offshore Guatemala	12°29.78'N, 91°02.26'W	4140	*D. neonautica* var. *cocosensis*	pl. 3, figs 9, 10	*B. d. n.* f. *cocosensis*
Bukry (1982b)	68	503A	EEP	4°04.04'N, 95°38.21'W	3672	*D. neonautica*	pl. 2, fig. 10; pl. 3, figs 1, 2	*B. d. n.* f. *neonautica*
						D. transenna n. sp.	pl. 4, figs 1-12	*B. d. n.* f. *transcenna*
Bukry (1983)	69	504	offshore Ecuador	1°13.58'N, 83°43.93'W	3460	*D. neonautica* var. *cocosensis*	pl. 4, fig. 7	*B. d. n.* f. *cocosensis*
						D. transenna	pl. 6, figs 2-4	*B. d. n.* f. *transcenna*
Locker and Martini (1986)	90	591	Southwest Pacific	31°35.06'S, 164°26.92'E	2131	*Neonaviculopsis* n. gen. *neonautica* f. *neonautica*	pl. 10, figs 6-11	*B. d. n.* f. *neonautica*
						Neonaviculopsis n. gen. *neonautica* f. *praenautica*	pl. 10, figs 1-5	*B. d. n.* f. *praenautica*
McCartney *et al.* (1995)	138	see Tab. 1	EEP	see Table 1	see Tab. 1	*B.d.n.* f. *cocosensis* n. f.	pl. 1, fig. 4; pl. 8, fig. 7	*B. d. n.* f. *cocosensis*
						Neonaviculopsis f. *neonautica*		*B. d. n.* f. *neonautica*
						B. d. n. f. *transenna* n. f.	pl. 1, figs 2, 3	*B. d. n.* f. *transcenna*
						Neonaviculopsis f. *praenautica*	pl. 1, fig. 7	*B. d. n.* f. *praenautica*

Table 2. List of the plexid morphogroups discussed in this paper, presented in the order of original description, with taxonomic synonyms.

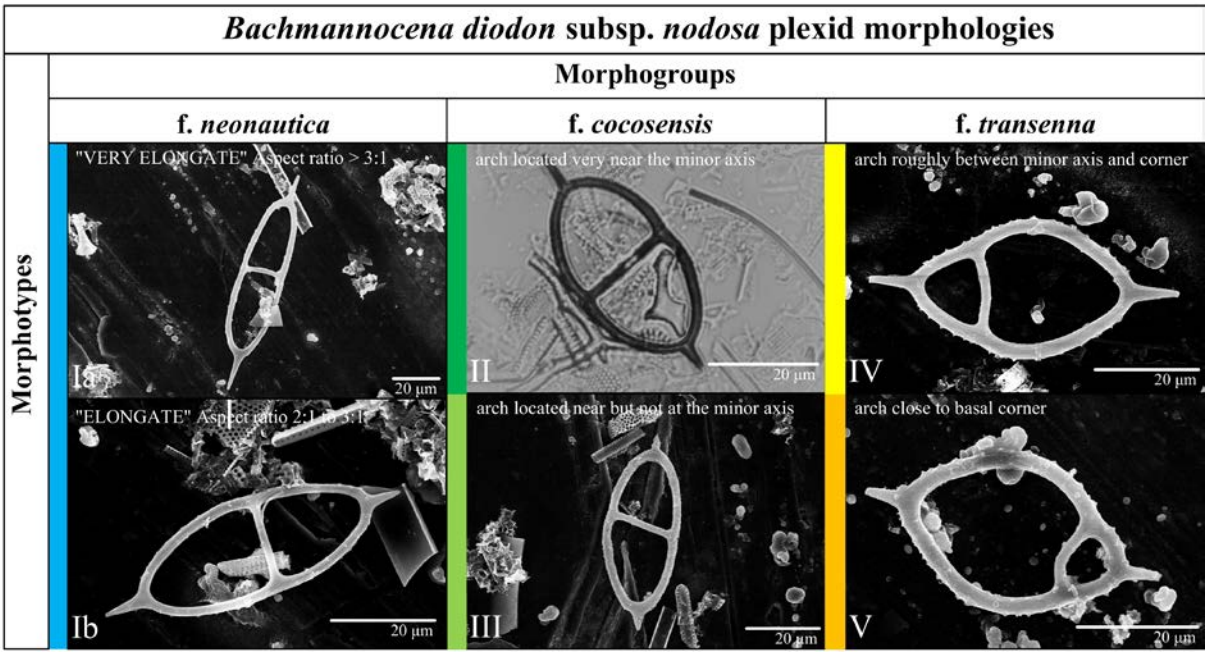

Text-fig. 3. Representative specimens of six BDN plexid morphologies counted in this study; Ia. 'very elongate' f. *neonautica*; Ib. 'elongate' f. *neonautica*; II. 'low' f. *cocosensis*; III. 'high' f. *cocosensis*; IV. 'low' f. *transenna*; V. 'high' f. *transenna.* The colors shown to the left of each photo indicate the predominance of this morphotype in Tables 3 to 7.

(1986) and McCartney *et al.* (1995). For cases like the recent usage of varieties by Malinverno *et al.* (2016) for modern silicoflagellate variation observed in the Mediterranean and Black Seas, we suggest that 'varieties' be consistently applied to the general variation associated with all silicoflagellates, while 'forms' (or *formae*) be used in reference to plexid morphologies (see Locker and Martini 1986).

For BDN f. *neonautica*, the arch is near the minor axis between basal corners and a distinction was made between basal rings identified as *elongate*, with basal aspect ratio 2:1 to 3:1, or *very elongate* with >3:1 ratio. BDN f. *praenautica*, with a bridge and four struts, was rarely observed in McCartney *et al*. (1995) and this study. Both f. *neonautica* and f. *praenautica* were placed in the new genus *Neonaviculopsis* by Locker and Martini (1986) as forms within *N. neonautica* subsp. *neonautica*. We

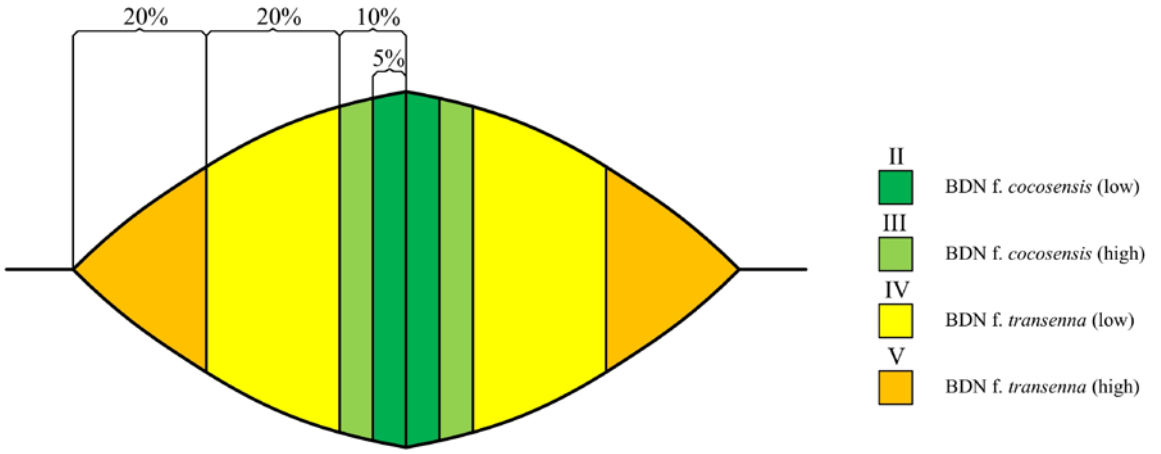

Text-fig. 4. Drawing showing the divisions between the low f. *cocosensis*, high f. *cocosensis*, low f. *transenna*, and high f. *transenna* morphotypes.

interpret these skeletal morphologies as part of the BDN plexus and thus within *Bachmannocena* (see discussion below).

The BDN f. *cocosensis* and f. *transenna* plexids have a basal aspect ratio <2:1 and were separated according to the arch location relative to the minor axis. These were identified according to the approximate 'latitudinal' position with respect to the minor axis (= equator), with positions determined as the percentage distance from minor axis to corner (= pole). Specimens counted as BDN f. *cocosensis* have the arch located within 20% of the distance between the minor axis to basal corner, while f. *transenna* have the arch closer to one corner (Text-fig. 4). Each of the f. *cocosensis* and f. *transenna* morphogroups is further separated into two morphotypes, with *low* being

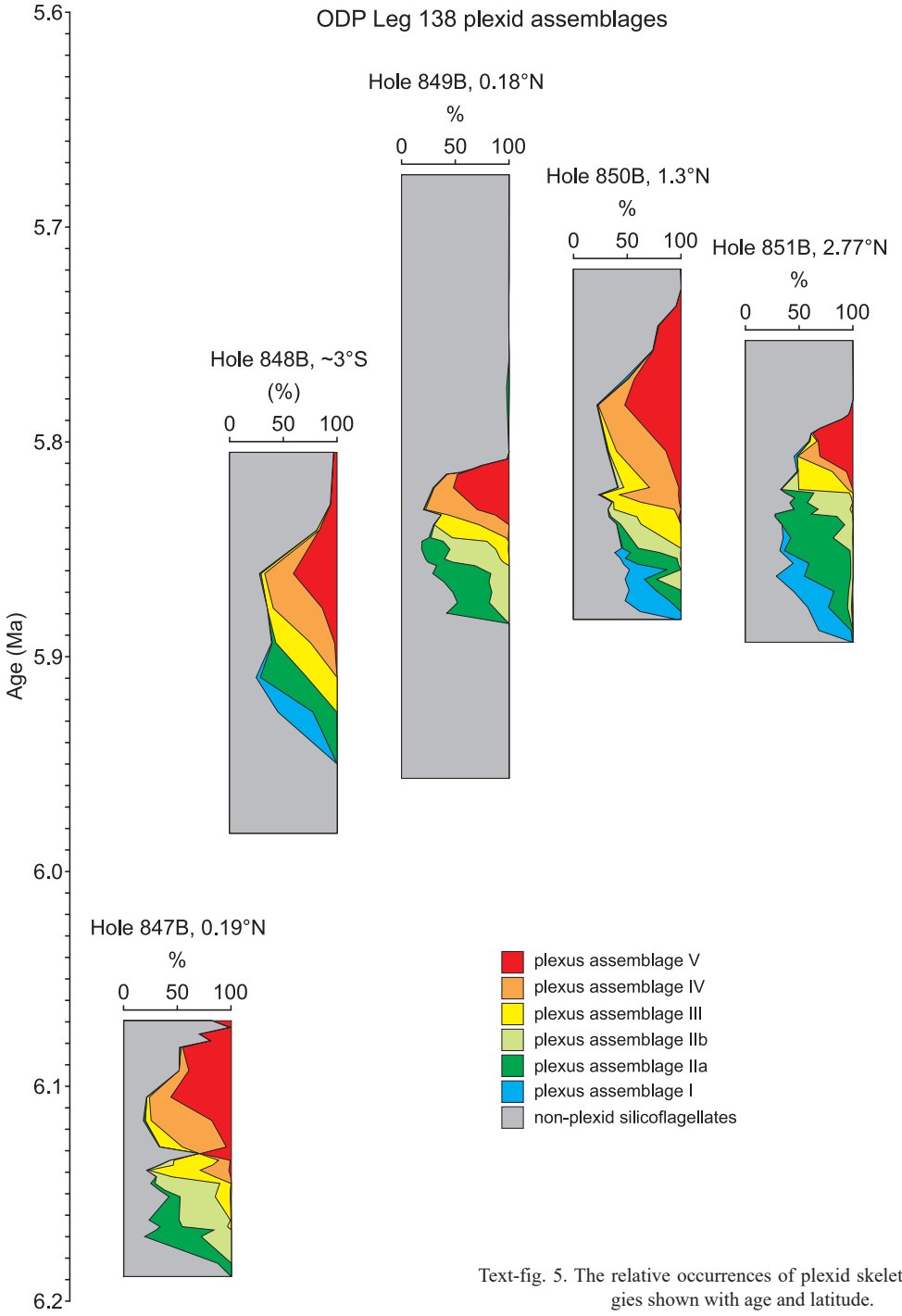

Text-fig. 5. The relative occurrences of plexid skeletal morphologies shown with age and latitude.

IODP Sample Number 138-847B	mbsf	mcd	Age	Plexid Interval	*Bachmannocena* sp.	*Dictyocha* sp.	*Stephanocha* sp.	Total non plexus silicoflagellates	*B. d. n. var. neonautica* (elong.)	*B. d. n. var. neonautica* (v. elong.)	*B. d. n. var. cocosensis* (low)	*B. d. n. var. cocosensis* (high)	*B. d. n. var. transcenna* (low)	*B. d. n. var. transcenna* (high)	*Bachmannocena diodon* subsp. *nodosa*	Total plexus silicoflagellates	Total silicoflagellates
138-847-B-22X-2, 120–121	195.9	215.3	6.069			134	112	246							54	54	300
138-847-B-22X-2, 140–141	196.1	215.5	6.073		6	166	122	294	1	1					4	6	300
138-847-B-22X-3, 10–11	196.3	215.7	6.076			109	101	210						1	89	90	300
138-847-B-22X-3, 30–31	196.5	215.9	6.079	VI		150	90	240						2	58	60	300
138-847-B-22X-3, 50–51	196.7	216.1	6.082			82	73	155		4			1	4	136	145	300
138-847-B-22X-3, 120–121	197.4	216.8	6.093			77	77	154						27	119	146	300
138-847-B-22X-4, 50–51	198.2	217.6	6.105			29	34	63		1			8	59	169	237	300
138-847-B-22X-4, 120–121	198.9	218.3	6.116	V		23	31	54	4		1	1	17	168	55	246	300
138-847-B-22X-5, 50–51	199.7	219.1	6.128			33	66	99			1	1	63	122	14	201	300
138-847-B-22X-5, 70–71	199.9	219.3	6.131	VI		118	92	210						4	86	90	300
138-847-B-22X-5, 90–91	200.1	219.5	6.134	IV		77	51	128			1	11	125	31	4	172	300
138-847-B-22X-5, 105–106	200.3	219.7	6.137			42	56	98			3	37	110	47	5	202	300
138-847-B-22X-5, 120–121	200.4	219.8	6.139			26	37	63				7	144	79	7	237	300
138-847-B-22X-5, 140–141	200.6	220.0	6.142			29	61	90			1	43	121	43	2	210	300
138-847-B-22X-6, 10–11	200.8	220.2	6.145	III		21	54	75			12	181	32			225	300
138-847-B-22X-6, 30–31	201.0	220.4	6.148			66	33	99			15	147	37	2		201	300
138-847-B-22X-6, 50–51	201.2	220.6	6.151			50	76	126			31	98	43	1	1	174	300
138-847-B-22X-6, 120–121	201.9	221.3	6.162			10	60	70	1		83	143	3			230	300
138-847-B-22X-6, 140–141	202.1	221.5	6.165			42	59	101			62	126	11			199	300
138-847-B-22X-7, 5–6	202.2	221.6	6.167			56	34	90			161	49				210	300
138-847-B-22X-7, 20–21	202.4	221.8	6.170	II		11	47	58			158	84				242	300
138-847-B-23X-1, 40–41	203.2	222.6	6.182			128	134	262	12	4	22					38	300
138-847-B-23X-1, 80–81	203.6	223.0	6.189			142	157	299			1					1	300

Table 3. Abundance counts of silicoflagellates in the late Miocene of Hole 847B. Interval I = BDN f. *neonautica*, Interval II = low f. *cocosensis*, Interval III = high f. *cocosensis*, Interval IV = low f. *transenna*, Interval V = high f. *transenna*, and Interval VI = f. *nodosa.*

closer to the minor axis and *high* closer to the corner. The arch of the low BDN f. *cocosensis* morphotype is within 10% of the distance from the minor axis and for the high morphotype it is between 10% to 20% of that distance (Text-fig. 4). For the low BDN f. *transenna* morphotype, the arch is between 20% to 60% and for high morphotype it is between 60% and near 100% of the distance (i.e., within 40% of the distance closest to the corner).

The very elongate f. *neonautica*, elongate f. *neonautica*, low and high f. *cocosensis*, low and high f. *transenna*, and nonplexid f. *nodosa* are identified respectively as morphotypes Ia, Ib, II, III, IV, V and VI in the range charts.

MATERIALS AND METHODS

Sample and slide preparation, photography

The samples were placed in 60 ml plastic containers, freeze-dried for 26 h, and subsequently pro-

IODP Sample Number	mbsf	mcd	Age		*Bachmannocena* sp.	*Dictyocha* sp.	*Stephanocha* sp.	Total non plexus silicoflagellates	*B. d. n. var. Neonautica* (elong.)	*B. d. n. var. neonautica* (v. elong.)	*B. d. n. var. cocoensis* (low)	*B. d. n. var. cocoensis* (high)	*B. d. n. var. transcemna* (low)	*B. d. n. var. transcemna* (high)	*Bachmannocena diodon* subsp. *nodosa*	Total plexus silicoflagellates	Total silicoflagellates
138-848B-7H-4, 50–51	54.7	61.40	5.805	VI		214	76	290							10	10	300
138-848B-7-H-4, 80–81	55.0	61.70	5.829		14	186	81	281				1			18	19	300
138-848B-7-H-4, 95–96	55.2	61.85	5.841			166	77	243					7		50	57	300
138-848B-7H-4, 120–121	55.4	62.10	5.861			71	6	77	1	3		3	4	80	102	193	270
138-848B-7-H-4, 140–141	55.6	62.30	5.877	V		68	37	105				5	12	137	41	195	300
138-848B-7-H-5, 10–11	55.8	62.50	5.894	IV		59	58	117		2	10	27	70	67	7	183	300
138-848B-7-H-5, 30–31	56.0	62.70	5.910	II	1	32	41	74	9	3	130	84				226	300
138-848B-7H-5, 50–51	56.2	62.90	5.926	I		92	41	133	48	52	66	1				167	300
138-848B-7H-5, 80–81	56.5	63.20	5.950			194	106	300								0	300
138-848B-7H-5, 120–121	56.9	63.60	5.982			216	84	300								0	300

Table 4. Abundance counts of silicoflagellates in the late Miocene of Hole 848B. Interval I = BDN f. *neonautica*, Interval II = low f. *cocosensis*, Interval III = high f. *cocosensis*, Interval IV = low f. *transenna*, Interval V = high f. *transenna*, and Interval VI = f. *nodosa*.

cessed following the random settling method outlined in Witkowski *et al*. (2012). Light (LM) and scanning electron microscopy (SEM) and microphotography equipment are described in McCartney *et al.* (2018).

Counting plexid skeletal morphologies

The focus of this study is the plexid occurrences, and hence other silicoflagellate taxa (primarily *Dictyocha* spp. and *Stephanocha* spp.) were identified only to genus level. Distinctions between the plexid morphotypes are presented above. Silicoflagellates in the plexid episode were often abundant enough that three hundred specimens could be counted from a single slide portion, with record made of the fraction of slide examined to show relative abundance (see McCartney *et al.* 1995). Specimens recorded in McCartney *et al.* (1995) as *Neonaviculopsis* Locker and Martini, 1986 are interpreted here as part of the BDN plexus and counted as BDN f. *neonautica* or f. *praenautica*.

Chronology

Determination of geologic age is based on cyclostratigraphic age models from Shackleton *et al*. (1995b). Age for the plexus inception and duration as well as sediment thickness of any specific intervals are determined as midpoints between observed samples that mark a transition. The age of individual samples was established by linear interpolation, assuming constant sedimentation rates (see McCartney *et al*. 2018).

RESULTS

To better understand the BDN plexus, a total of 222 sediment samples from Holes 844B, 847B, 848B, 849B, 850B, 851B and 852B were examined, with the silicoflagellates of 114 samples counted to establish the interval boundaries shown below. The BDN plexus morphotypes occur at Holes 847B, 848B, 849B, 850B and 851B (Tables 3–7, respectively) but were not observed at Holes 844B and 852B, where 11 and 37 samples respectively were processed and microscope slides examined.

Among the four holes of the N-S transect (848B, 849B, 850B and 851B), the initiation age of the episode is fairly consistent at about 5.9 Ma, with the beginning at Hole 850B being less precise because the bottom is not bounded by a non-plexid sample. This is remarkably consistent, considering that only a small fraction of biostratigraphic datums from the main microfossil groups are demonstrably synchronous (<0.1 myr) over the Leg 138 study area (Shackleton *et al.* 1995a, p. 529). The termination age for the plexus episode shows greater variation, but the average is about 5.842 Ma (±0.027 myr). Hole

IODP Sample Number	mbsf	mcd	Age	Plexid Interval	*Bachmannocena* sp.	*Dictyocha* sp.	*Stephanocha* sp.	Total non plexus silicoflagellates	*B. d. n. var. neonautica* (elong.)	*B. d. n. var. neonautica* (v. elong.)	*B. d. n. var. cocoensis* (low)	*B. d. n. var. cocoensis* (high)	*B. d. n. var. transcenna* (low)	*B. d. n. var. transcenna* (high)	*Bachmannocena diodon* subsp. *nodosa*	Total plexus silicoflagellates	Total silicoflagellates
138-849B-19X-2, 121–122	168.7	195.1	5.676		6	145	149	300								0	300
138-849B-19X-3, 120–121	171.2	197.6	5.722		10	146	143	299				1				1	300
138-849B-19X-4, 121–122	172.7	199.1	5.744			179	120	299							1	1	300
138-849B-19X-5, 121–122	174.2	200.6	5.761		3	184	113	300								0	300
138-849B-19X-6, 121–122	175.7	202.1	5.775		23	172	98	293			7					7	300
138-849B-20X-1, 21–22	177.9	206.8	5.804		11	231	57	299							1	1	300
138-849B-20X-1, 45–46	178.1	207.0	5.805		4	173	123	300								0	300
138-849B-20X-1, 121–122	178.9	207.8	5.808		14	169	111	294						1	5	6	300
138-849B-20X-2, 45–46	179.6	208.5	5.811			98	126	224				1		1	74	76	300
138-849B-20X-2, 80–81	180.0	208.9	5.813			87	111	198						4	98	102	300
138-849B-20X-2, 120–121	180.4	209.3	5.814	VI		98	66	164		2				8	126	136	300
138-849B-20X-2, 140–141	180.6	209.5	5.815			63	62	125					3	28	144	175	300
138-849B-20X-3, 45–46	181.1	210.0	5.821			50	38	88				1	2	54	155	212	300
138-849B-20X-3, 120–121	181.9	210.8	5.832	V		22	39	61		1		1	4	145	88	239	300
138-849B-20X-3, 140–141	182.1	211.0	5.834			82	28	110					21	131	38	190	300
138-849B-20X-4, 45–46	182.6	211.5	5.839	IV		30	59	89	1		2		125	83		211	300
138-849B-20X-4, 120–121	183.4	212.3	5.845			18	58	76	1		5	60	150	6	2	224	300
138-849B-20X-4, 140–141	183.6	212.5	5.846	III		22	35	57			59	122	61	1		243	300
138-849B-20X-5, 41–42	184.1	213.0	5.850			35	21	56			79	128	35	2		244	300
138-849B-20X-5, 101–102	184.7	213.6	5.855			21	46	67	3		50	156	24			233	300
138-849B-20X-5, 121–122	184.9	213.8	5.856			12	62	74	5	1	63	141	16			226	300
138-849B-20X-5, 140–141	185.1	214.0	5.858	II		36	62	98			107	95				202	300
138-849B-20X-6, 41–42	185.6	214.5	5.861			38	49	87	21		141	51				213	300
138-849B-20X-6, 81–82	186.0	214.9	5.865			56	62	118	12		114	56				182	300
138-849B-20X-6, 101–102	186.2	215.1	5.870			72	71	143	18	12	79	48				157	300
138-849B-20X-6, 121–122	186.4	215.3	5.875			87	69	156	12	10	67	55				144	300
138-849B-20X-6, 140–141	186.6	215.5	5.880			70	56	126	46	19	81	28				174	300
138-849B-20X-7, 20–21	186.8	215.7	5.885			176	124	300								0	300
138-849B-21X-1, 10–11	187.4	216.3	5.903			183	117	300								0	300
138-849B-21X-1, 20–21	187.5	217.4	5.957			160	140	300								0	300

Table 5. Abundance counts of silicoflagellates in the late Miocene of Hole 849B. Interval I = BDN f. *neonautica*, Interval II = low f. *cocosensis*, Interval III = high f. *cocosensis*, Interval IV = low f. *transenna*. Interval V = high f. *transenna*, and Interval VI = f. *nodosa.*

847B, located ~15º E of the N-S transect and closer to South America, has later ages of episode initiation and termination at ~6.19 and 6.11 Ma, respectively.

Where the plexus episode was observed during the course of this study, a succession of sediment intervals occurs with each dominated by a single plexid morphotype. These intervals are identified here according to the predominant morphotype and shown in Tables 3–7. The bottom of the plexus episode begins with a predominance of f. *neonautica,* with the elongate morphotype being usually most abundant. Stratigraphically above the f. *neonautica* interval, morphologies possess a less elongate basal ring with an arch at or near the minor-axis (f. *cocosensis*), with the arch gradually moving towards a basal corner (f. *transenna*) over time, ending with the predominant f. *nodosa*. The sequence with time is consistently f. *neonautica*, low f. *cocosensis*, high f. *cocosensis*, low f. *transenna*, high f. *transenna*, to f. *nodosa*.

IODP Sample Number	mbsf	mcd	Age	Plexid Interval	*Bachmannocena* sp.	*Dictyocha* sp.	*Stephanocha* sp.	Total non plexus silicoflagellates	*B. d. n. var. neonautica* (elong.)	*B. d. n. var. neonautica* (v. elong.)	*B. d. n. var. cocosensis* (low)	*B. d. n. var. cocosensis* (high)	*B. d. n. var. transcenna* (low)	*B. d. n. var. transcenna* (high)	*Bachmannocena diodon* subsp. *nodosa*	aberrant	Total plexus silicoflagellates	Total silicoflagellates
138-850B-16X2, 40–41	148.0	155.5	5.765		8	124	166	298						1	1		2	300
138-850B-16X-2, 121–122	148.8	156.3	5.775		16	168	116	300									0	300
138-850B-16X-3, 40–41	149.5	157.0	5.783	VI	16	151	119	286							14		14	300
138-850B-16X-3, 121–122	150.3	150.3	5.723			131	104	235				1		2	62		65	300
138-850B -16X4, 40–41	151.0	158.5	5.802			140	81	221						2	77		79	300
138-850B-16X-4, 121–122	151.8	159.3	5.815			59	84	143	1	7			2	17	130		157	300
138-850B-16X-5, 40–41	152.5	160.0	5.827			19	46	65		1		1	2	74	157		235	300
138-850B-16X-5, 121–122	153.3	160.8	5.845	V		45	49	94	1	1		2	22	138	42		206	300
138-850B-16X-6, 40–41	154.0	161.5	5.866			49	74	123			2	15	72	82	6		177	300
138-850B-16X-6, 60–61	154.2	161.7	5.869			38	32	70			4	2	52	165	7		230	300
138-850B-16X-6, 80–81	154.4	161.9	5.873			42	65	107			1	4	75	108	5		193	300
138-850B-16X-6, 100–101	154.6	162.1	5.876	IV		48	48	96				17	168	19			204	300
138-850B-16X-6, 121–122	154.8	162.3	5.879			33	66	99			6	72	114	3	5	1	201	300
138-850B-16X-6, 140–141	155.0	162.5	5.883			44	76	120			11	57	111	1			180	300
138-850B-17X-1, 5–6	155.8	163.3	5.895	III		33	101	134	3		44	119					166	300
138-850B-17X-1, 21–22	155.9	163.4	5.897	II		22	93	115	37	7	82	58	1				185	300
138-850B-17X-1, 40–41	156.1	163.6	5.900			44	87	131	11	3	144	10	1				169	300
138-850B-17X-1, 60–61	156.3	163.8	5.902			57	83	140	39	1	113	7					160	300
138-850B-17X-1, 80–81	156.5	164.0	5.905	I		85	69	154	69	37	39	1					146	300
138-850B-17X-1, 100–101	156.7	164.2	5.908			78	66	144	54		34	68					156	300
138-850B-17X-1, 120–121	156.9	164.4	5.911			90	65	155	72	2	70	1					145	300
138-850B-17X-1, 140–141	157.1	164.6	5.917			73	71	144	124		32						156	300
138-850B-17X-2, 20–21	157.3	164.8	5.922			121	65	186	95	19							114	300
138-850B-17X-2, 40–41	157.5	165.0	5.926			205	81	286	12	2							14	300

Table 6. Abundance counts of silicoflagellates in the late Miocene of Hole 850B. Interval I = BDN f. *neonautica*, Interval II = low f. *cocosensis*, Interval III = high f. *cocosensis*, Interval IV = low f. *transenna*, Interval V = high f. *transenna*, and Interval VI = f. *nodosa.*

The study sites differ in the stratigraphic completeness of the plexus episode succession. The complete succession occurs at Hole 850B (Table 6). Hole 851B lacks a predominant high f. *transenna* interval, but that morphology is abundant enough in the two subjacent observed samples to indicate an occurrence in the ~0.01 myr between these (Table 7). Similarly in Hole 848B, where the entire episode was only 0.85 m, a predominant high f. *cocosensis* was abundant enough in the two subjacent samples (Table 4) to infer an occurrence in the ~0.02 myr separation. Holes 847B and 849B lack a predominant f. *neonautica* interval with ~0.007 and ~0.005 myr, respectively, between the lowest plexid and highest non-plexid samples (Tables 3 and 5).

The age extent, calculated using mid-points between boundary samples, is shown for each hole in Text-fig. 5. Of the four holes on the N-S transect, sediment thicknesses of the episode in Holes 851B, 850B and 849B were 380, 461 and 520 cm, respectively. The highest observed sedimentation rate, ~70.3 cm/myr, was in Hole 849B, which is the modern location closest to the equator. The southernmost site of this study (Hole 848B) was much thinner, at 85 cm, and had the lowest sedimentation rate, at ~12.5 m/myr, explained by the location being furthest from the equatorial divergence. Thus, the plexus appears to be thickest near the equator, and to rapidly thin away from that latitude. The later ages of episode initiation and termination at Hole 747B is possibly explained by the equatorial current system being moved from the direct influence of the eastern

IODP Sample Number	mbsf	mcd	Age	Plexid Interval	*Bachmannocena* sp.	*Praenautica* sp.	*Dictyocha* sp.	*Stephanocha* sp.	Total non plexus silicoflagellates	*B. d. n. f. neonavicula* (elong.)	*B. d. n. f. neonavicula* (v. elong.)	*B. d. n. f. cocosensis* (low)	*B. d. n. f. cocosensis* (high)	*B. d. n. f. transcenna* (low)	*B. d. n. f. transcenna* (high)	*Bachmannocena diodon* subsp. *nodosa*	aberrant	Total plexus silicoflagellates	Total silicoflagellates
138-851B-12H-5, 120–121	109.7	124.7	5.753		8		221	70	299							1		1	300
138-851B-12H-6, 120–121	111.2	126.2	5.774		5		177	118	300									0	300
138-851B-12H-7, 20–21	111.7	126.7	5.780		2		167	131	300									0	300
138-851B-12H-7, 40–41	112.1	127.1	5.785	VI	12		187	94	293							7		7	300
138-851B-12H-7, 60–61	112.3	127.3	5.787		18		177	93	288							12		12	300
138-851B-12H-7, 78–79	112.5	127.5	5.789				201	68	269							31		31	300
138-851B-13H-1, 5–6	112.1	127.1	5.784				149	58	207		1					92		93	300
138-851B-13H-1, 20–21	112.2	127.2	5.786		1		133	38	172		11				6	111		128	300
138-851B-13H-1, 40–41	112.4	128.2	5.800				91	86	177	1	2			20	3	97		123	300
138-851B-13H-1, 80–81	112.8	128.6	5.8067				62	74	136	6	2			2	62	92		164	300
138-851B-13H-1, 120–121	113.2	129.0	5.8138	IV			82	62	144	3				95	40	18		156	300
138-851B-13H-2, 45–46	113.9	129.7	5.822				43	55	98			2	49	138	13			202	300
138-851B-13H-2, 59–60	114.0	129.8	5.824	III			69	42	111			80	99	10				189	300
138-851B-13H-2, 80–81	114.2	130.0	5.826				58	79	137			45	114	4				163	300
138-851B-13H-2, 100–101	114.4	130.2	5.828				47	77	124			49	126	1				176	300
138-851B-13H-2, 120–121	114.7	130.5	5.831				43	92	135			68	89	6	2			165	300
138-851B-13H-2, 140–141	114.9	130.7	5.834				23	60	83			101	115	1				217	300
138-851B-13H-3, 5–6	115.0	130.8	5.835	II			27	55	82			173	44	1				218	300
138-851B-13H-3, 25–26	115.2	131.0	5.839				49	53	102			175	23					198	300
138-851B-13H-3, 45–46	115.4	131.2	5.845				52	61	113	22	1	127	58	1				187	300
138-851B-13H-3, 60–61	115.6	131.4	5.851				49	47	96	13		183	8					204	300
138-851B-13H-3, 80–81	115.8	131.6	5.857				56	77	133	40	4	117	6					167	300
138-851B-13H-3, 100–101	116.0	131.8	5.863				45	41	86	58	21	129	6					214	300
138-851B-13H-3, 120–121	116.2	132.0	5.870	I			94	40	134	45	68	41	10			2		166	300
138-851B-13H-3, 145–146	116.4	132.2	5.877			2	82	78	162	65	5	50	14	3	1			138	300
138-851B-13H-4, 20–21	116.7	132.5	5.888				103	102	205	61	29	5						95	300
138-851B-13H-4, 45–46	116.9	132.7	5.893				169	130	299		1							1	300

Table 7. Abundance counts of silicoflagellates in the late Miocene of Hole 851B. Interval I = BDN f. *neonautica*, Interval II = low f. *cocosensis*, Interval III = high f. *cocosensis*, Interval IV = low f. *transenna*, Interval V = high f. *transenna*, and Interval VI = f. *nodosa.*

boundary currents (Raffi and Flores 1995, p. 255). The N-S observed geographic extent of the plexus is less than 6º latitude.

DISCUSSION

Paleoceanographic context

The BDN plexus occurs in a short interval of the upper Miocene (silicoflagellate zone *Dictyocha extensa*, McCartney *et al.* 1995; nannoplankton zone NN11b/CN9bC, Raffi and Flores 1995; diatom zone *Thalassiosira convexa*, Baldauf and Iwai 1995; radiolarian zone *Stichocorys peregrina*, Moore 1995) near the top of the *Bachmannocena diodon* range. The temporal extent of the plexus episode, at c. 5.9–5.84 Ma, occurs roughly at the boundary between an oxygen isotope low and inception of the Messinian Oxygen Isotope High at 5.9 Ma (Drury *et al.* 2016). The plexus occurs late in the Messinian Salinity Crisis (5.96–5.33 Ma) associated with glacio-eustatic sea-level variations (Ohneiser *et al.* 2015) and near the beginning of a global late Miocene cooling trend (~7.5–6 Ma, Herbert *et al.* 2016). This time is also near the end of a steep decline in atmospheric and

oceanic CO_2 concentrations, as shown by a recent detailed study of the past 13 myr CO_2 record (Mejía *et al.* 2017), but such observations do not explain the particular occurrences of these quite unusual silicoflagellate skeletal morphologies.

This plexus occurs within a time of particularly high though variable sediment accumulation, especially near the equator, that reflects sedimentation recovery after a 'carbonate crash' centered at ~9.5 Ma (Farrell *et al.* 1995). A portion of this high sedimentation can be attributed to laminated diatom mats, with rates of 100 to >150 m/myr (Kemp 1995, p. 629). However, significant laminated diatom oozes were not observed during the temporal interval covered by the BDN plexus, as shown by Pearce *et al.* (1995, p. 649). Sediment rates calculated from the present study vary from a low of ~12 (Hole 848B) to 70 (Hole 849B) m/myr.

Silicoflagellate plexus episodes include unusual skeletal morphologies, often in great abundance, that are assumed to mark a time when the ability to take on such shapes placed the species at a competitive advantage, either with other silicoflagellates or the phytoplankton population as a whole (McCartney and Wise 1990). While the *nodosa* plexus shows unusual skeletal morphologies, the variability at any given time within the episode is constrained so that a specific morphotype often predominates. We think this implicates some external environmental factor that may have been most pronounced in the Eastern Equatorial Pacific, a location that would be associated with relatively warm waters and high upwelling.

The ~6 Ma BDN plexus episode occurred at a time of significant tectonic events elsewhere that may be related to glacio-eustatic changes associated with the Messinian Salinity Crisis (Ohneiser *et al.* 2015). While the closure of the Central American Seaway likely occurred after the interval of our study, the Bering Strait gateway connected the North Pacific and Arctic Oceans at about this time, which influenced changes in marine surface salinity through freshwater atmospheric transport (Brierley and Federov 2016). As suggested by Bukry (1987), the Peru Current may have had a particular influence on the presence of *Bachmannocena* taxa.

Significance of *nodosa* morphologies

The late Miocene to early Pliocene was also a time of significant changes in the relative abundance of other silicoflagellate skeletal morphologies. A shift from minor-axis to major-axis bridge alignments occurs among *Dictyocha* that appeared gradually over the late Miocene (McCartney *et al.* 1995). The approximate time of the BDN plexus marked an evolutionary divergence between *D. stapedia* Haeckel, 1887 and *D. perlaevis* Frenguelli, 1951, as shown by the presence of transitional morphologies (*Dictyocha* sp. at Site 751B, McCartney *et al.* 1995). An acme of *Paramesocena* also occurred in the late Miocene to early Pliocene (Perch-Nielsen 1975; Bukry 1986, Table 1), but these species were not abundant in the Eastern Equatorial Pacific (Bukry and Foster 1973; McCartney *et al.* 1995). Also in this general temporal interval are extensive pennate diatom mats in the Equatorial Pacific but also in the much more northern (~45º N) ODP Sites 885/886 (Dickens and Barron 1997).

The BDN plexid morphologies are especially unusual, even by the standards of silicoflagellate high diversity and variability, for several reasons. To begin, the abundant presence of apical arches associated with BDN is unique in the known history of *Bachmannocena*. Furthermore, the abundant occurrence of an apical structure not centered above the middle of the basal ring, as observed for BDN f. *transenna*, is virtually unique for silicoflagellates, the notabilid morphology among the pseudofibulid plexa of *Stephanocha speculum* and *Dictyocha grandis* (see McCartney and Wise 1990; Witkowski *et al.* 2012) being another example of an eccentric apical morphology.

The occurrence of arched BDN and the transitional movement above the basal plane must have an explanation, for which we can only provide speculation. Mathematical modeling by McCartney and Loper (1989) suggested that an important function of the apical structure is to support the outer cell surface to reduce surface energy during the divisional process (McCartney *et al.* 2014). The general history of naviculopsid silicoflagellates indicates that there may have times when there was a need for apical elements to divide the apical cell wall into small portals (McCartney *et al.* 2020). A smaller overall skeletal size may achieve this as well. Note that the overall size of f. *nodosa* associated with the plexid interval are smaller than *Bachmannocena* in general.

The general lack of an apical structure on *Bachmannocena* skeletons suggests that a centralization of cell material may not be as important for the mesocenids compared to other silicoflagellates during division. However, some combination of long-term low CO_2 levels (Mejía *et al.* 2017), change in regional upwelling, or precipitation conditions (Brierley and Federov 2016) and increased continental weathering (Dickens and Barron 1997) associated with condi-

tions of ocean/atmosphere dynamics that enhanced productivity may have favored the occurrence of an apical structure among these *Bachmannocena* taxa during the BDN plexus episode.

Taxonomic placement

We conclude that the BDN plexid morphologies, placed by various workers in the genera *Dictyocha*, *Neonaviculopsis* and *Bachmannocena* (Table 1), are closely related and thus should collectively be considered as plexus variation in a single genus and species. *Neonaviculopsis* is excluded as genus for this group, in part because the generic description only includes *Neonaviculopsis neonautica* subsp. *neonautica* Locker and Martini, 1986 and *N. neonautica* subsp. *praenautica* Locker and Martini, 1986, but also because we show this to be part of larger variation associated with an earlier-described genus. There is, we think, stronger evidence for placement in either *Dictyocha* or *Bachmannocena*, with evidence weighted to the latter.

Dictyocha fibula subsp. *ausonia* (Deflandre) McCartney, Churchill and Woestendiek, 1995 occurs above, below, and within the plexus (McCartney *et al*. 1995); some of the illustrated specimens in that paper (McCartney *et al*. 1995, pl. 2, figs 3, 4) have strut attachments near enough to the minor axis to be connected by a single element without the usual triple junction at the corner, and one illustrated specimen (McCartney *et al*. 1995, pl. 5, fig. 4) has an arch offset to one major-axis corner (see also Bukry 1980, pl. 1, figs 11–14). These specimens are evidence for *Dictyocha* as a progenitor of the BDN plexid morphotypes. The co-occurrence of the *ausonia* and *praenavicula* morphologies with similar long bridges with short struts, may be related by evolutionary or ecologic factors, and so is deserving of further study.

The placement of the plexid morphologies within BDN (McCartney *et al.* 1995) was due to the close physical similarities of basal ring size and surface ornamentation, particularly between f. *cocosensis* and f. *transenna*, and *Bachmannocena diodon*. The surface texture and corner spine placement of the BDN skeletons both within and stratigraphically above the plexus interval are closely similar to *B. diodon* basal rings from earlier in the Miocene, and thus we continue the taxonomic placement within *Bachmannocena*. Whether the evolutionary heritage be *Dictyocha* or *Bachmannocena*, the abundance and transition of these morphologies through the plexus interval is unusual and thus of particular note to the silicoflagellate paleontologist.

CONCLUSIONS

- Skeletal morphologies of the *Bachmannocena diodon* subsp. *nodosa* plexus occur in a regular stratigraphic sequence, beginning with morphotypes that have an arch across the minor axis. Over the subsequent several tens of kyr, the arch moved towards a basal corner. The sequence ends with *Bachmannocena diodon* subsp. *nodosa* f. *nodosa,* a mesocenid morphology that lacks apical structure.
- The skeletal morphotypes of the *Bachmannocena diodon* subsp. *nodosa* plexus include forms that were previously placed in *Neonaviculopsis*. Since no additional taxa have been placed in this species, *Neonaviculopsis* is now considered a junior synonym of *Bachmannocena*.

NEW COMBINATIONS

Bachmannocena diodon nodosa f. *neonautica* (Locker and Martini) McCartney and Szaruga, comb. nov.

BASIONYM: *Neonaviculopsis neonautica neonautica* Locker and Martini, 1986, p. 909, pl. 10, figs 6–11.

Bachmannocena diodon nodosa f. *praenautica* (Locker and Martini) McCartney and Szaruga, comb. nov.

BASIONYM: *Neonaviculopsis neonautica praeneonautica* Locker and Martini, 1986, p. 909, pl. 10, figs 1–5, 12.

Acknowledgements

We thank the International Ocean Discovery Program and in particular Phil Rumford for providing samples from other legs for comparative study. We also thank Jere Lipps and Richard A. Jordan for detailed reviews of the manuscript and Anna Żylińska for further edits. This work initiated by a sabbatical from the University of Maine at Presque Isle and University of Maine System and award of a Fulbright Fellowship to KMc in 2016–2017, and was continued during an additional sabbatical and Kościuszko Fellowship in 2019 to KMc. This study was supported by National Science Centre grant no. 2014/13/B/ST10/02988 to JW.

REFERENCES

Baldauf, J.G. and Iwai, M. 1995. Neogene diatom biostratigraphy for the eastern equatorial Pacific Ocean, Leg 138. *Pro-*

ceedings of the Ocean Drilling Program, Scientific Results, **138**, 105–128.

Brierley, C.M. and Fedorov, A.V. 2016. Comparing the impacts of Miocene–Pliocene changes in inter-ocean gateways on climate: Central American Seaway, Bering Strait, and Indonesia. *Earth and Planetary Science Letters*, **444**, 116–130.

Bukry, D. 1980. Miocene *Corbisema triacantha* Zone phytoplankton from Deep Sea Drilling Project Sites 415 and 416, off Northwest Africa. *Initial Reports of the Deep Sea Drilling Project, Scientific Results*, **50**, 507–523.

Bukry, D. 1981a. Silicoflagellate stratigraphy of offshore California and Baja California, Deep Sea Drilling Project Leg 63. *Initial Reports of the Deep Sea Drilling Project, Scientific Results*, **67**, 539–557.

Bukry, D. 1981b. Synthesis of silicoflagellate stratigraphy for Maastrichtian to Quaternary marine sediment. *SEPM Special Publication*, **32**, 433–444.

Bukry, D. 1982a. Cenozoic silicoflagellates from offshore Guatemala, Deep Sea Drilling Project Site 495. *Initial Reports of the Deep Sea Drilling Project, Scientific Results*, **67**, 425–445.

Bukry, D. 1982b. Neogene silicoflagellates from the eastern equatorial Pacific, Deep Sea Drilling Project Hole 503A. *Initial Reports of the Deep Sea Drilling Project, Scientific Results*, **68**, 311–323.

Bukry, D. 1983. Upper Cenozoic silicoflagellates from offshore Ecuador, Deep Sea Drilling Project Site 504. *Initial Reports of the Deep Sea Drilling Project, Scientific Results*, **69**, 321–342.

Bukry, D. 1986. Miocene silicoflagellates from Chatham Rise, Deep Sea Drilling Project Site 594. *Initial Reports of the Deep Sea Drilling Project, Scientific Results*, **90**, 925–937.

Bukry, D. 1987. Eocene siliceous and calcareous phytoplankton, Deep Sea Drilling Project Leg 95. *Initial Reports of the Deep Sea Drilling Project, Scientific Results*, **95**, 815–871.

Bukry, D. and Foster, J.H. 1973. Silicoflagellate and diatom stratigraphy, Leg 16, Deep Sea Drilling Project. *Initial Reports of the Deep Sea Drilling Project, Scientific Results*, **16**, 395–415.

Dickens, G.R. and Barron, J. 1997. A rapidly deposited pennate diatom ooze in Upper Miocene–Lower Pliocene sediment beneath the North Pacific polar front. *Marine Micropaleontology*, **31**, 177–182.

Drury, A.J, John, C.M. and Shevenell, A.E. 2016. Evaluating climatic response to external radiative forcing during the late Miocene to early Pliocene. New perspectives from eastern equatorial Pacific (IODP U1338) and North Atlantic (ODP 982) locations. *Paleooceanography*, **31**, 167–184.

Ehrenberg, C.G. 1843. Einige vorläufige Resultate der Untersuchungen der von der Südpolreise des Capitain Ross, so wie in den Herren Schayer und Darwin zugekommenen Materialien über das Verhalten des kleinsten Lebens in den oceanen und den grössten bisher zugänglichen Tiefen des Weltmeers vor. *Berichte über die zur Bekanntmachung geeigneten Verhandlungen der Königlich-Preussischen Akademie der Wissenschaften zu Berlin*, **1844**, 182–207.

Farrell, J.W., Raffi, I., Janecek, T.R., Murray, D.W., Levitan, M., Dadey, K.A., Emeis, K.C., Lyle, M., Flores, J.A. and Hovan, S. 1995. Late Neogene sedimentation patterns in the Eastern Equatorial Pacific Ocean. *Proceedings of the Ocean Drilling Program, Scientific Results*, **138**, 717–756.

Frenguelli, J. 1935. Variaciones de *Dictyocha fibula* en el Golfo de San Matías. *Annales del Museo Argentino de Ciencias Naturales*, **38**, 263–381.

Frenguelli, J. 1951. Silicoflagelados del Trípoli de Mejillones (Chile). *Physis*, **20**, 272–284.

Jordan, R.W. and McCartney, K. 2015. Stephanocha nom. nov., a replacement name for the illegitimate silicoflagellate genus *Distephanus* Stöhr. *Phytotaxa*, **201**, 177–187.

Haeckel, E. 1887. Report on the radiolarians collected by H.M.S. Challenger during the years 1873–1876. *Reports of the Scientific Results of H.M.S. Challenger during the years 1873–1876*, **18**, 1803 pp.

Herbert, T.D., Lawrence, K.T., Tzanova, A., Peterson, L.C., Caballero-Gill, R. and Kelly, C.S. 2016. Late Miocene global cooling and the rise of modern ecosystems. *Nature Geoscience*, **9**, 843–847.

Kemp, A.E.S. 1995. Origins and paleoceanographic significance of laminated diatom ooze from the Eastern Equatorial Pacific Ocean. *Proceedings of the Ocean Drilling Program, Scientific Results*, **138**, 641–645.

Locker, S. 1974. Revision der Silicoflagellaten aus der Mikrogeologischen Sammlung von C.G. Ehrenberg. *Eclogae geologicae Helvetiae*, **67**, 631–646.

Locker, S. and Martini, E. 1986. Silicoflagellates and some sponge spicules from the southwest Pacific, Deep Sea Drilling Project, Leg 90. *Initial Reports of the Deep Sea Drilling Project, Scientific Results*, **90**, 887–924.

Malinverno, E., Cerino, F., Karatsolis B.-T., Ravani, A., Dimiza, M. Psarra, S., Gogou, A. and Triantaphyllou, M. 2019. Silicoflagellates in the eastern Mediterranean and Black Seas: Seasonality, distribution and sedimentary record. *Deep-Sea Research Part II, Topical Studies in Oceanography*, **164**, 122–134.

Malinverno, E., Karatsolis, B.-T., Dimiza, M.D., Lagaria, A., Psarra, S. and Triantaphyylou, M.V. 2016. Extant silicoflagellates from the Northeast Aegean (eastern Mediterranean Sea): Morphologies and double skeletons. *Revue de Micropaléontologie*, **59**, 253–265.

McCartney, K. and Harwood, D.M. 1992. Silicoflagellates from Leg 120 on the Kerguelen Plateau, Southeast Indian Ocean. *Proceedings of the Ocean Drilling Program, Scientific Results*, **120**, 811–831.

McCartney, K. and Loper, D.E. 1989. Mathematical modeling of *Dictyocha* and *Distephanus* skeletal morphology. *Paleobiology*, **15**, 283–298.

McCartney, K. and Wise, S.W., Jr. 1990. Cenozoic silicoflagellates and ebridians from Ocean Drilling Program Leg 113: Biostratigraphy and notes on morphologic variability. *Proceedings of the Ocean Drilling Program, Scientific Results*, **113**, 729–760.

McCartney, K. and Wise, S.W., Jr. 1993. Unusual silicoflagellate skeletal morphologies from the upper Miocene–lower Pliocene: possible ecophenotypic variations from the high-latitude southern oceans. In: Kennett, J.P. and Warnke, D.A. (Eds), *The Antarctic Paleoenvironment: A Perspective on Global Change, Antarctic Research Series*, **60**, 195–206.

McCartney, K., Churchill, S. and Woestendiek, L. 1995. Silicoflagellates and ebridians from ODP Leg 138, Eastern Equatorial Pacific. *Proceedings of the Ocean Drilling Program, Scientific Results*, **138**, 129–162.

McCartney, K., Harwood, D.M. and Witkowski, J. 2011. Late Cretaceous silicoflagellate taxonomy and biostratigraphy of the Arctic Margin, Northwest Territories, Canada. *Micropaleontology*, **57**, 61–86.

McCartney, K., Witkowski, J., Jordan, R.W., Daugbjerg, N., Malinverno, E., van Wezel, R., Kano, H., Abe, K., Scott, F., Schweizer, M., Young, J.R., Hallegraeff, G.M. and Shiozawa, A. 2014. Fine structure of silicoflagellate double skeletons. *Marine Micropaleontology*, **113**, 10–19.

McCartney, K., Witkowski, J. and Szaruga, A. 2018. Paleocene–early Eocene Southern subtropical to subpolar silicoflagellate biostratigraphy. *Acta Geologica Polonica*, **68**, 219–247.

McCartney, K., Witkowski, J., Nowakowski, R., Szaruga, A., Wróbel, R. and Zgłobicka, I. 2020. Evolution of the silicoflagellate naviculopsid skeletal morphology in the Cenozoic. *Marine Micropaleontology*, **156**, 101820.

Mejía, L.M., Méndez-Vicente, A., Abrevaya, L., Lawrence, K.T., Ladlow, C., Bolton, C., Cacho, I. and Stoll, H. 2017. A diatom record of CO2 decline since the late Miocene. *Earth and Planetary Science Letters*, **479**, 18–33.

Moore, T.C., Jr. 1995. Radiolarian stratigraphy, Leg 138. *Proceedings of the Ocean Drilling Program, Scientific Results*, **138**, 191–232.

Ohneiser, C., Florindo, F., Stocchi, P., Roberts, A.P., DeConto, R.M. and Pollard, D. 2015. Antarctic glacio-eustatic contributions to late Miocene Mediterranean desiccation and reflooding. *Nature Communications*, **6**, 8765.

Perch-Nielsen, K. 1975. Late Cretaceous to Pleistocene silicoflagellates from the southern southwest Pacific, DSDP, Leg 29. *Initial Reports of the Deep Sea Drilling Project, Scientific Results*, **29**, 677–721.

Pearce, R.B., Kemp, A.E.S., Baldauf, J.G. and King, S.C. 1995. High-resolution sedimentology and micropaleontology of laminated diatomaceous sediments from the Eastern Equatorial Pacific Ocean. *Proceedings of the Ocean Drilling Program, Scientific Results*, **138**, 647–663.

Raffi, I. and Flores, J.-A. 1995. Pleistocene through Miocene calcareous nannofossils from eastern equatorial Pacific Ocean (Leg 138). *Proceedings of the Ocean Drilling Program, Scientific Results*, **138**, 233–289.

Shackleton, N.J., Baldauf, J.G., Flores, J.-A., Iwai, M., Moore, T.C., Jr., Raffi, I. and Vincent, E. 1995a. Biostratigraphic summary for Leg 138. *Proceedings of the Ocean Drilling Program, Scientific Results*, **138**, 517–536.

Shackleton, N.J., Crowhurst, S., Hagelberg, T., Pisias, N.G. and Schneider, D.A. 1995b. A new late Neogene time scale: Application to Leg 138 sites. *Proceedings of the Ocean Drilling Program, Scientific Results*, **138**, 73–101.

Shaw, C.A. and Ciesielski, P.F. 1983. Silicoflagellate biostratigraphy of middle Eocene to Holocene subantarctic sediments recovered by Deep Sea Drilling Project Leg 71. *Initial Reports of the Deep Sea Drilling Project, Scientific Results*, **71**, 687–737.

Shitanaka, M. 1983. Silicoflagellate remains in the sediments of Lake Haruga, Fukui, Japan. *Bulletin Mizunami Fossil Museum*, **10**, 171–180.

Takahashi, K., Onodera, J. and Katsuki, K. 2009. Significant populations of seven-sided *Distephanus* (Silicoflagellata) in the sea-ice covered environment of the central Arctic Ocean, summer 2004. *Micropaleontology*, **55**, 313–325.

Witkowski, J., Bohaty, S.M., McCartney, K. and Harwood, D.M. 2012. Enhanced siliceous plankton productivity in response to middle Eocene warming at Southern Ocean ODP Sites 748 and 749. *Palaeogeography*, *Palaeoclimatology*, *Palaeoecology*, **326–328**, 78–94.

Manuscript submitted: 18th August 2021
Revised version accepted: 19th October 2021